

Final Report: Vibration Analysis of a Loudspeaker via Michelson Interferometer

Yusuf Kayra Gül^{1,*}

¹*Department of Physics, Bilkent University, Ankara 06800, Türkiye*

(Dated: December 26, 2025)

In 1880, A. A. Michelson invented the well-known Michelson interferometer, which was later used in the Michelson–Morley experiment to test the existence of the aether. Although the experiment failed, the Michelson interferometer still has many applications, including the present experiment. Aim of this experiment is to observe the vibrations created by a loudspeaker using the modified version of well known Michelson Interferometer. Modification of the setup will be done by introducing a loudspeaker to the system, which will create vibrations via sound waves. Thus, the disturbance of interference pattern due to vibrations will enable us to detect those vibrations precisely. Implementing a FFT algorithm provide a determination of the distinct frequencies of the vibrations.

INTRODUCTION

Albert A. Michelson was a successful physicist who had done major contributions to optics in late 19th century, which is one of the fundamental areas of physics. Using the interferometer he designed, he achieved a highly accurate measurement of the speed of light in 1881. In 1887, together with Edward W. Morley, he conducted the well known Michelson–Morley experiment, which demonstrated the absence of detectable aether drift and played a key role in the development of special relativity [1].

Working principle of Michelson Interferometer is based on wave optics. The aim of the device is to detect interference and the diffraction patterns of light as the name implies. This mechanism enables us to measure several aspects of light or light related events[1] [2].

In this experiment classical Michelson Interferometer has modified using a loudspeaker instead of a static object. This modification introduce vibrations on one of the mirrors. This vibration of mirror has continuously altered the distance from the beam splitter thus changed the path difference. This alteration of the path difference created a vibration on the pattern which has captured and analyzed with FFT.

THEORY

Michelson Interferometer

The Michelson interferometer consists of a laser, a beam splitter, and two mirrors oriented perpendicular to each other. Light emitted from the laser is divided by the beam splitter into two beams with equal intensity. These beams propagate along perpendicular paths, are reflected by the mirrors, and meet at the beam splitter. Any difference in the optical path lengths of the two beams produces a phase difference, which determines whether the interference is constructive or destructive [3].

Constructive interference occurs when the optical path difference satisfies

$$\Delta d = d_2 - d_1 = n \frac{\lambda}{2}, \quad (1)$$

where d_1 and d_2 represent the distances between the beam splitter and the mirrors, λ is the wavelength of the light, and n is an integer [3].

The electric fields of the two interfering beams can be expressed as

$$E_1 = Ae^{i(\omega t + \phi_1)}, \quad (2)$$

$$E_2 = Ae^{i(\omega t + \phi_2)}, \quad (3)$$

where A is the amplitude, ω is the angular frequency, t denotes time, and ϕ_1 and ϕ_2 are the

phase constants. The total electric field is obtained by superposing two electric fields:

$$E = E_1 + E_2 = Ae^{i\omega t} (e^{i\phi_1} + e^{i\phi_2}). \quad (4)$$

The intensity is proportional to the squared magnitude of the total electric field,

$$\begin{aligned} |E|^2 &= EE^* \\ |E|^2 &= Ae^{i\omega t} (e^{i\phi_1} + e^{i\phi_2}) \times Ae^{-i\omega t} (e^{-i\phi_1} + e^{-i\phi_2}) \\ |E|^2 &= A^2 [e^0 + e^{i(\phi_1 - \phi_2)} + e^{i(\phi_2 - \phi_1)} + e^0] \\ |E|^2 &= A^2 (1 + 1 + e^{i(\phi_1 - \phi_2)} + e^{i(\phi_2 - \phi_1)}) \\ |E|^2 &= 2A^2(1 + \cos(\Delta\phi)) \end{aligned}$$

where $\Delta\phi = \phi_1 - \phi_2$ is the phase difference. Expressing this phase difference in terms of the optical path difference yields

$$|E|^2 = 2A^2 \left(1 + \cos \left(2\pi \frac{2\Delta d}{\lambda} \right) \right). \quad (5)$$

Since the response of photodetector is proportional to the light intensity, alterations in $|E|^2$ are expected to directly translate into measurable electrical signals [4].

In the modified configuration used in this experiment, one mirror is fixed while the other is mounted on a loudspeaker. The oscillatory motion of the loudspeaker induces periodic displacements of the mirror and modulating the optical path difference. If the mirror undergoes sinusoidal motion, the path difference can be approximated as

$$\Delta d \approx 2A \sin(\omega t), \quad (6)$$

where A is the displacement amplitude and ω is the angular frequency of the vibration. This periodic modulation causes the interference fringes to oscillate, producing a harmonic variation in the output of the photodetector. The resulting signal then can be analyzed using FFT techniques to determine vibration frequencies [5].

Discrete Fourier Transform

Fourier analysis is used to find the frequency components. For a data $x[n]$ with N data points, the Discrete Fourier Transform (DFT) is defined as

$$X[k] = \sum_{n=0}^{N-1} x[n] e^{-i2\pi kn/N}, \quad (7)$$

where k is the frequency index and magnitude $|X[k]|$ shows the amplitude of each frequency component. The direct evaluation of the DFT scales as $\mathcal{O}(N^2)$ and becomes inefficient for large data sets. The Fast Fourier Transform (FFT) uses the symmetry in the exponential factors to reduce the complexity to $\mathcal{O}(N \log N)$ while staying mathematically equivalent to the DFT [6]. Due to vast number of data points acquired in this experiment, analysis of these data will be done using FFT.

Diverging Lens

Diverging (concave) lenses are used in the optical setup to expand the laser beam and enhance the visibility of the interference pattern. When parallel rays enter a diverging lens, they spread outward as if originating from the focal point on the same side of the lens [7].

Assume an incident laser beam of radius r . Then the relationship between the incoming and outgoing beam radii can be derived using similar triangles. If r' denotes the beam radius at a distance d from the lens and f is the focal length, the angle α satisfies:

$$\tan \alpha = \frac{2r}{f} = \frac{2r'}{f+d}. \quad (8)$$

Defining the magnification factor M as the ratio of beam radii, $M = r'/r$, yields:

$$M = \frac{r'}{r} = \frac{f+d}{f}. \quad (9)$$

This expression shows that the beam expansion increases with the distance between the

lens and the screen, allowing the interference fringes to be observed more clearly [7].

METHODOLOGY

The interferometer part of the experimental setup consists of a 532 nm green laser as a light source, a beam splitter, 2 mirrors, a loudspeaker as source of vibration. Also several diverging and converging lenses are used to magnify the pattern. Furthermore, the setup has built on a heavy granite slab standing on 4 seismic isolators to reduce external vibrations which would affect the data negatively as noise.

To capture the data; a photodetector with an amplifier composed of a BPW 34 S photodiode, TLV2462 Op Amp, proper resistors and capacitors connected to an Arduino Uno has used.

A sketch of the experimental setup and an actual image of the setup are provided below.

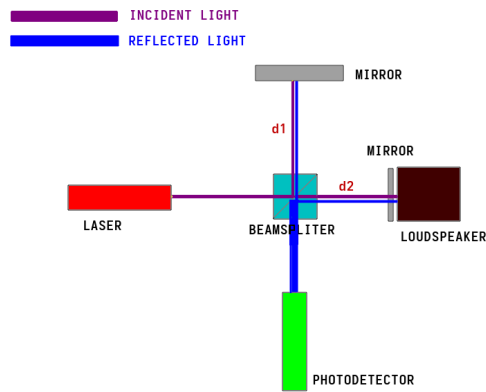


FIG. 1. A demonstration of the setup consisting of a laser, beam splitter, loudspeaker, two mirrors, and a photo detector.

As it could be seen lenses used to magnify the pattern are not included here but they are in actual setup which is as follows:



FIG. 2. An image of the actual setup consisting mentioned equipments for interferometer.

1. A Michelson Interferometer has built using the mentioned equipments. Beam splitter has placed on the diagonal of two mirrors with a $\pi/2$ angle in between. Incoming laser beam has splitted into two separate beams via beam splitter which are then reflected back from mirrors and meet again on beam splitter. This meeting of the beams created an interference pattern due to path differences of two beams, which altered via the vibrations of loudspeaker.
2. The vibrations has introduced to the system via a loudspeaker placed as in Figure 2. The distinct frequencies has created using MATLAB codes to create sound via sine waves. It should be noted that amplitude of the applied sound should be as low as possible since the aim is to vibrate just one mirror not whole the system. This acquired by simply turning down the volume consistently until the measurements became sufficiently consistent with the given vibrations.
3. The alteration of the pattern could be seen with naked eye. Furthermore it could also be analyzed by a photo detector to determine the vibration frequency of the pattern which is expected to match vibration frequency of the loudspeaker.
4. The photo detector has constructed using the components mentioned earlier. The BPW 34 S has a spectral range

of sensitivity for wavelengths between 420nm - 1120nm which was suitable for the laser pointer used in the setup with 532nm wavelength. Furthermore, mentioned photodiode has a response time around $\sim 20\text{ns}$ which provide photo detector to capture high frequency alterations in the pattern [8].

5. An amplifier circuit including TLV2462 Op Amp, $1\text{ M}\Omega$ resistor and 100nF capacitor has included into the photodetector to amplify the signal created by photodiode. The output of the photodiode has amplified from $0\text{V} - 0.2\text{V}$ to $0 - 5.0\text{V}$ via the amplifier circuit.
6. The photodetector has built on a breadboard and connected to an Arduino Uno to capture data. The code has written in a way that Arduino to capture $\sim 3.8 \times 10^4$ data points per second. The captured data then transferred into Python to run an FFT and plot. Also some of the data acquired were from recordings of the complex sounds such as musics and conversations which converted back to sound with appropriate filtering techniques to reconstruct the sound applied to the system

RESULTS

In the experiment, a clear and stable interference pattern has acquired. An image of one of the patterns acquired with setup shown in Figure 2 is as follows:

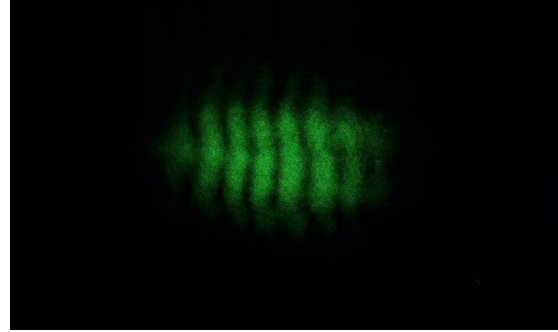


FIG. 3. One of the patterns used in experiment.

Throughout the project, different patterns has acquired. Nevertheless, shape of the pattern does not affect the results since experiment aims to capture and analyze vibrations and alterations of the pattern not the actual shape.

So, various types of sounds are introduced to the setup as vibrations via loudspeaker which also vibrate the pattern. These vibrations can be separated into two sections: Distinct Frequencies and Complex Frequencies. Here distinct frequencies represents vibrations consists of at most 3 distinct sine waves and complex frequencies represents sound recordings such as musics and conversations which consists a spectra of frequencies.

Results for Distinct Frequencies

In this part of the experiment various sine waves with various frequencies has created and converted into sound using MATLAB. The sound produced by MATLAB then introduced to the system via laudspeaker. The data has captured for 20 s then analysed with a FFT algorithm.

First, single sine wave sounds with distinct frequencies are introduced to the system. The intensity data collected by photodetector has passed through an FFT analysis with Hann Windowing and plotted to compare with given frequency.

For this part vibrations of 400 Hz and 1000

Hz are introduced separately in different runs with different measurements. The results are provided below.

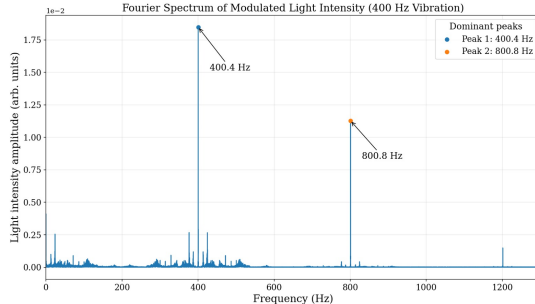


FIG. 4. The FFT analysis of the data collected with a vibration of 400 Hz is applied.

Figure 4 clearly shows a peak at 400.4 Hz which is sufficiently consistent with the introduced vibration of 400 Hz. Also there are other peaks at integer multiples of 400 Hz caused by both convolution in FFT and harmonic distortion which will be discussed in Error Analysis section.

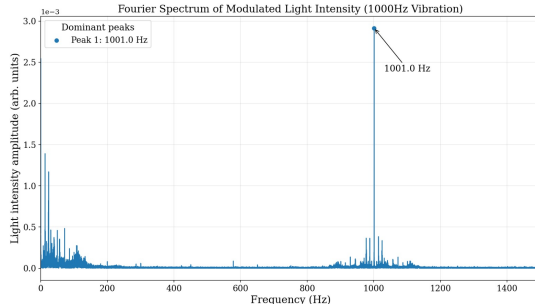


FIG. 5. The FFT analysis of the data collected with a vibration of 1000 Hz is applied.

Figure 5 shows a distinct peak at 1001.0 Hz which is sufficiently consistent with the introduced vibration of 1000 Hz. The interesting thing is that both 400 Hz and 1000 Hz measurements has an error of exactly 0.1 percent which also could be a consequence of the har-

monic distortion or the spacing of the grid used while FFT.

Secondly, two sine wave sounds with different frequencies are introduced simultaneously to the system and analyzed in the same way.

For this part, vibrations of 400 Hz and 600 Hz frequencies are introduced simultaneously. The result is provided below.

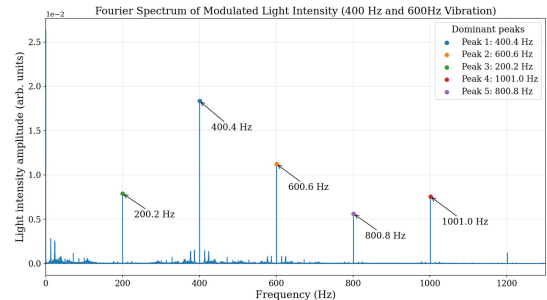


FIG. 6. The FFT analysis of the data collected with vibrations of 400 Hz and 600 Hz are applied.

As Figure 6 shows the highest peaks present are at 400.4 Hz and 600.6 Hz which are greatly consistent with the introduced vibrations of 400 Hz and 600 Hz. Unfortunately, due to more vibration in the system noise and effect of both harmonic distortion and convolution has increased.

Finally, three sine wave sounds with different frequencies are introduced simultaneously to the system and also analyzed in the same way.

For this final part, two measurements has taken. One with vibrations of 400 Hz, 600 Hz, and 1000 Hz. Other with frequencies of 50 Hz, 2000 Hz, and 5000 Hz. The second measurement was to test the systems response when high and low frequencies introduced simultaneously. The results are provided below again.

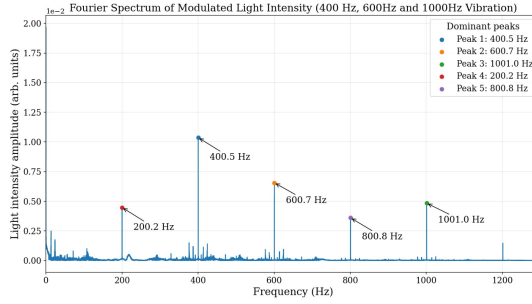


FIG. 7. The FFT analysis of the data collected with vibrations of 400 Hz, 600 Hz, and 1000 Hz are applied.

As Figure 7 shows, there are complements of the given frequencies in the FFT plot at 400.5 Hz, 600.7 Hz, and 1001.0 Hz. 400.5 Hz and 600.7 Hz are clearly consequences of the vibration introduced to the system but since 1001.0 Hz also appears in Figure 6 it is not clear that if 1001.0 Hz is a consequence of convolution, harmonic distortion or the actual vibration introduced to the system. Although, the system should have been capture the 1000 Hz frequency as Figure 5 implies. Thus, probably the peak at 1001.0 Hz in Figure 7 is a consequence of all convolution, harmonic distortion and actual vibration in the system.

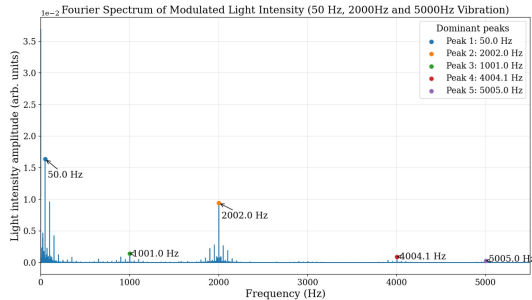


FIG. 8. The FFT analysis of the data collected with vibrations of 50 Hz, 2000 Hz, and 5000 Hz are applied.

Since this measurement is to see the limits of the setup, it has observed that the response at

5005.0 Hz is extremely low compared with the responses at 50.0 Hz and 2002.0 Hz as Figure 8 implies. Nevertheless, it could be said that the peak at 5005.0 Hz is not a consequence of integer multiples of introduced frequencies since it is neither an integer multiple of 50.0 Hz nor 2002.0 Hz. Thus, setup is able to capture relatively high frequencies but with lower amplitudes. Also, setup captures the low frequencies very efficiently.

As the results imply, the system is sufficient for determining single, double, and triple frequencies applied simultaneously. Nevertheless, errors and the unwanted peaks at integer multiples of the actual frequencies present in every measurement due to harmonic distortion and convolution in FFT.

Result for Complex Frequencies

In this part of the experiment, sound waves of a music record have introduced to the system via loudspeaker. The data has captured for 20 s and the same FFT analysis is applied to the data. Also, an FFT has applied to same 20 s of the music record introduced to system. The comparison of the results are as follows:

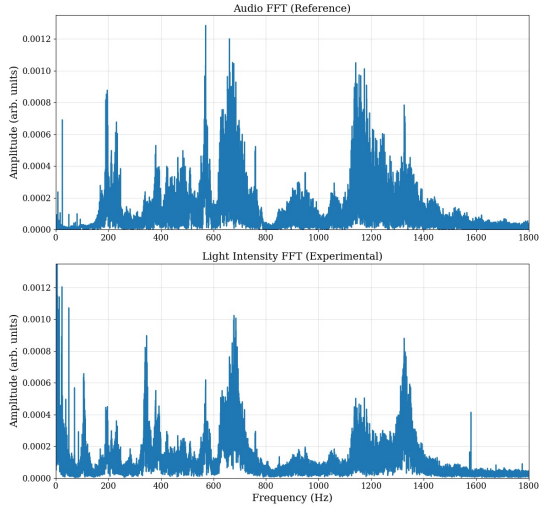


FIG. 9. The FFT analysis of the data collected with a sound recording is introduced and the FFT analysis of the actual audio.

The general shape of the experimental result is consistent with the audio reference as Figure 9 clearly demonstrates. Nevertheless, the amplitude proportions between frequencies are slightly off due to both noise and imperfections of FFT.

The acquired data also reconstructed as audio to compare with actual audio. Unfortunately adding mentioned audios to this report is not possible but as the result provided in Figure 9 implies, reconstructed audio and the actual audio were greatly consistent with each other with a slight noise.

ERROR ANALYSIS

Since the interferometer has tried to be built with low budget equipments, it has limitations.

One of these limitations is that imperfect insulation of external vibration which causes noise and error in the data even though a granite slab with 4 seismic isolators used. With more professional equipments such as optic rails or optical table one could greatly reduce the effect of ex-

ternal vibrations.

In addition, the laser used has an inhomogeneous beam which has a constant pattern consist of bright and dark areas instead of a homogeneous circular shape due to lack of quality of the laser. A laser specifically designed for optic experiments could have more homogeneous beam which results in more precise measurements of the interference pattern.

Furthermore, the optical equipments used such as glass slide, converging lenses, and diverging lenses were not ideal as expected. The glass slide was not splitting the laser beam perfectly 1/1 ratio but absorbing some of it which cause a slight decrease in intensity of the outgoing beam. Also the converging and diverging lenses were not perfect either, the reflections created by the lenses greatly reduced the intensity of pattern acquired. All these reductions of the light intensity caused response of the photodiode to be reduced which leads noise to be more effective. Using high quality and professional equipments would prevent this intensity reduction effect.

Several nonlinear effects may have occurred while the loudspeaker vibrates the system which cause given frequency to differ in output. These nonlinear effects create harmonic distortion which cause the unwanted peaks at integer multiples of introduced actual frequencies and also the mentioned exact and consistent 0.1 percent deviation of the results [9].

Since setup is used to record data for finite time periods, this finite time period acted as a step function multiplied with the actual data. Thus, in FFT analysis the data has seen as convolution of mentioned step function and actual data. This caused the presence of integer multiples of actual frequencies in the FFT analysis plots. Recording data for a much longer time would reduce the effect of convolution, but due to data capturing at high rate with Arduino and transferring it via USB cable to computer created lack of synchronization for long records which made taking longer records impossible with current equipments.

Also, the discrete grid used in FFT and finite sampling rate of the photodetector and Arduino affected the results. Better equipments which could acquire higher sampling rate and a FFT algorithm which uses finer grids would reduce the error.

CONCLUSION

The results of the experiment mostly met with the expectations. For the relatively lower frequencies (50 Hz - 2000 Hz) the response of the setup is much more than the response it gives for the relatively high frequencies (5000 Hz) as Figure 8 and Figure 7 implies. Furthermore due to high measurement rate around $\sim 3.8 \times 10^4$ data points per second, the setup was sufficient to capture high frequencies even though the response is lower than low frequencies. This behavior can be explained by the response of the loudspeaker mirror system and the limitations of the photodetector. In conclusion, a modified version of Michelson Interferometer has built in order to conduct a vibration analysis of a loudspeaker and since the ultimate aim of the experiment was to determine frequencies introduced by loudspeaker to the system accurately, the results show that the project successfully achieved its aim. With improved external vibration isolation and higher-quality components, the sensitivity and frequency range of the system could

be further enhanced in future projects.

* kayra.gul@ug.bilkent.edu.tr

- [1] A. Lucas, *Albert A. Michelson and his Interferometer: Lord of the Spinning Worlds, Master of Light* (Cambridge Scholars Publishing, 2023) pp. 6–22.
- [2] P. Hariharan, *Optical Interferometry*, 2nd ed. (Academic Press, 2003) Chap. 1.
- [3] F. A. Jenkins and H. E. White, *Fundamentals of Optics* (McGraw-Hill, 1976) pp. 271–276.
- [4] J. Crawford, Frank S., Introduction and superposition of harmonic waves, in *Waves: Berkeley Physics Course, Volume 3* (McGraw-Hill, New York, 1968) pp. 403–495.
- [5] J. Baker, R. Laming, T. Wilmhurst, and N. Halliwell, A new, high sensitivity laser vibrometer, *Optics Laser Technology* **22**, 241 (1990).
- [6] A. L. Garcia, *Numerical Methods for Physics* (Prentice Hall, Englewood Cliffs, NJ, 2000) Chap. 5.2, pp. 153–162.
- [7] E. Hecht, *Optics*, 5th ed. (Pearson Education, Boston, 2017) pp. 159–182.
- [8] OSRAM Opto Semiconductors, BPW 34 S Silicon PIN Photodiode, <https://look.ams-osram.com/m/1f206a499ac1f0b2/original/BPW-34-S.pdf> (2021), datasheet, Version 1.7, Accessed: 2024-10-27.
- [9] R. P. Feynman, R. B. Leighton, and M. Sands, *The Feynman Lectures on Physics, Vol. I* (Addison-Wesley, 1963) Chap. 50.